Supplementary Material

Edu Proliferation Assay

Primary tumor tissue was dissociated and tumor cells were cultured in NeuroCult Basal Medium (Stemcell, 05700) supplemented with NeuroCult Proliferation Supplement (Stemcell, 05701), EGF [20ng/mL], FGF [20ng/mL], and Heparin (0.25%). 75,000 or 100,000 Single cells were plated as a monolayer in 12 well plates coated with vitronectin (Corning Synthemax, 89235-046), accutased at designated time points, and then the Click-iT Plus Edu Kit (Invitrogen, C10636) was used according to manufacturer's protocol. Cells were then run on a BD-LSR II flow cytometer and analyzed in FlowJo.

Cytokine Array

Snap frozen tumor tissue was homogenized and lysed in 1x PBS lysis buffer containing 1% Triton, 10µg/mL Aprotinin (Sigma, A6279), 10µg/mL Leupeptin (Sigma, L8511), and 10µg/mL Pepstatin (Sigma, P4265). 500µg of pooled sample protein was used according to manufacturer's instructions for the Mouse Cytokine Array Panel A (R&D Systems, ARY006). The blot was developed and visualized via HRP. Densitometry quantification was performed in ImageJ Fiji.

Enzyme Linked Immunosorbent Assay

Snap frozen tumor tissue was mechanically homogenized and sonicated in lysis buffer supplemented with protease and phosphatase inhibitors. Cell lysates were subjected to sonication in supplemented lysis buffer. Protein concentrations were determined using a Bradford protein assay (BioRad, 5000001). ELISA assays were performed for CCL2 (R&D, DY-479), CCL7 (Boster, EKO683), CCL8 (R&D, DY790), CCL12 (R&D, MCC120) and VEGFA (R&D, MMV00) according to the manufacturer's instructions

Human RNA Sequencing

The following has been adapted from (Mackay *et al.*, 2017). mRNA gene expression data was obtained from Agilent WG2.5, Affymetrix U133Plus2.0 or RNA sequencing platforms. Gene expression was processed from two color Agilent microarrays using the R packages marray and limma and from single channel Affymetrix arrays using the affy package. Differential expression was assigned for microarray data using the limma package based upon a false discovery rate of

5%. RNASeq was aligned with Bowtie2 and TopHat and summarized as gene level fragments per kilobase per million reads sequenced using BEDTools and cufflinks/cuffnorm. Following rlog transformation and normalization, differential expression was assigned with DESeq.2. Known Ensembl genes were further filtered to remove low abundance genes in all three datasets whose maximal expression was within the lowest 20% of all expression values based upon probe intensities or read depth. Replicate probes/features for each gene were removed by selecting those with the greatest median absolute deviation (MAD) in each dataset. Following centering within each dataset, log-transformed expression measures were combined and further normalized using pairwise loess normalization.

BMDM and Microglia Cell Cultures

BMDMs and microglia were isolated and cultured as previously described (Herting *et al.*, 2019; Chen *et al.*, 2020). Briefly, bone marrow was isolated from adult CL57BL/6 mice and cells were cultured at 37^{o}C for 6 days in DMEM high glucose culture medium (Gibco, 10569-010) supplemented with 10% FBS, 1X L-glutamine, 1X Penicillin/Streptomycin, and M-CSF (40ng/mL). On day 7 post isolation, 2 million cells/well were plated in a 6 well tissue culture treated plate and incubated overnight. The next morning cells were incubated in FBS deficient media (0.5%) for 3 hours and then stimulated with recombinant human PDGFA (0-100ng/mL; R&D Systems) or PDGFB (0-100 ng/mL; R&D Systems) for 6 hours. RNA was collected using Trizol (ThermoFisher) added directly to the tissue culture plate and then stored at -80^{o}C.

Microglia were isolated from CL57BL/6 pups aged 0-2 days old and plated on a poly-D-lysine coated (10 mg/mL) T75 flask in DMEM high glucose media containing M-CSF (40ng/mL). Approximately 10 days later, microglia were gently rinsed off the flask and 1 million cells/well were then plated on a 6-well tissue culture treated plate overnight. Cells were then incubated in FBS deficient media for 3 hours prior to stimulation with PDGFA or PDGFB as described above.

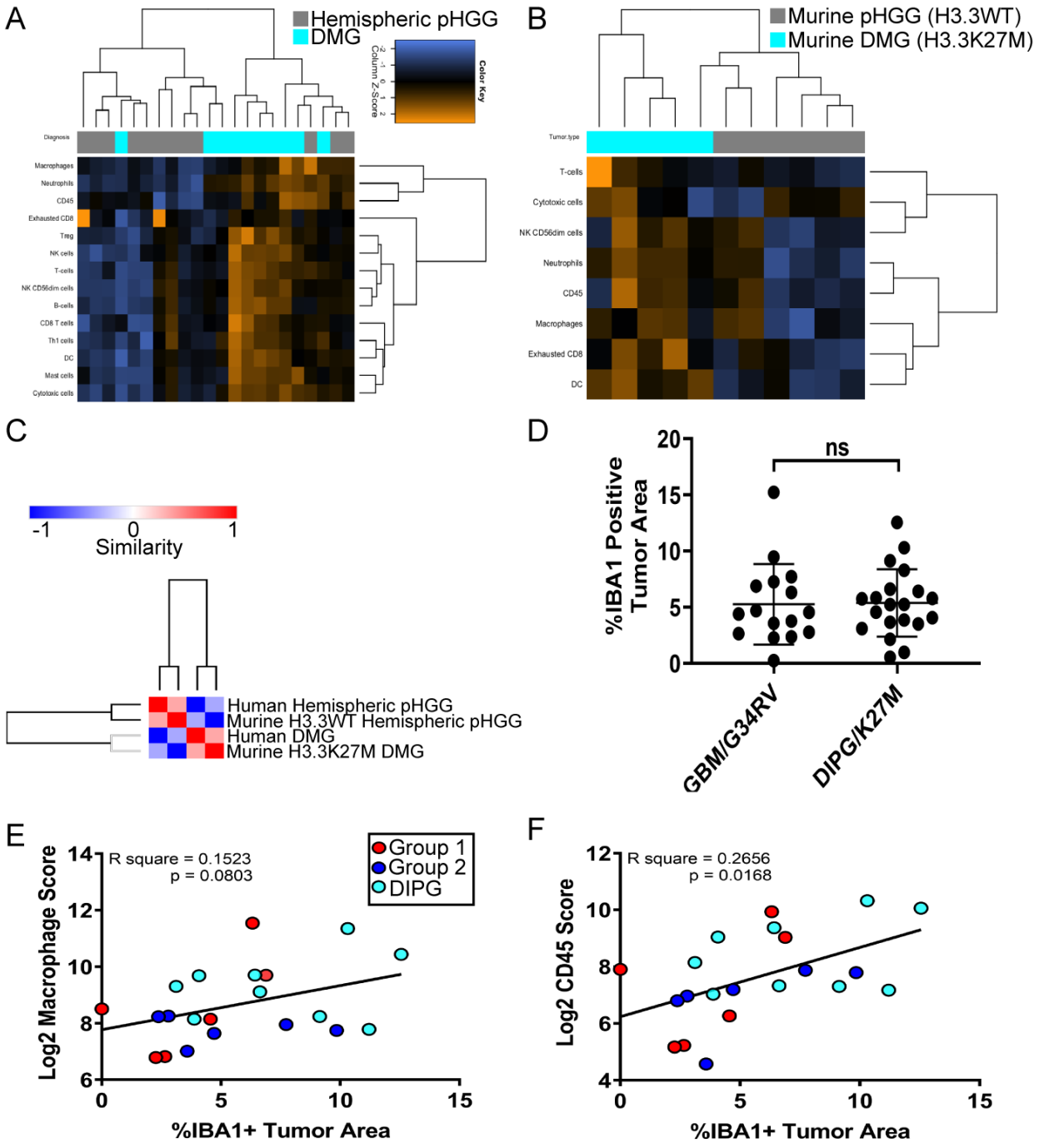

Figure 1. (A) Unsupervised hierarchical clustering of cell type scores obtained from NanoString on human pHGGs and on **(B)** bulk tumor tissue from H3.3WT Hemispheric pHGGs (n=5) or H3.3K27M DIPGs (n=5) in *Ntva;Cdkn2a-/-* mice. **(C)** Similarity matrix of human hemispheric pHGG and DMG, and murine hemispheric pHGG and DMG, clustered by similarity based on the expression of all detected genes in the NanoString panel. **(D)** Quantification of IBA1 staining in human pHGG samples, separated by molecular subtype (GBM/H3G34RV mutant vs

DIPG/H3K27M mutant). **(E)** Macrophage Score and **(F)** CD45 Scores obtained from NanoString correlated with %IBA1+ staining in matched human samples. n=21.

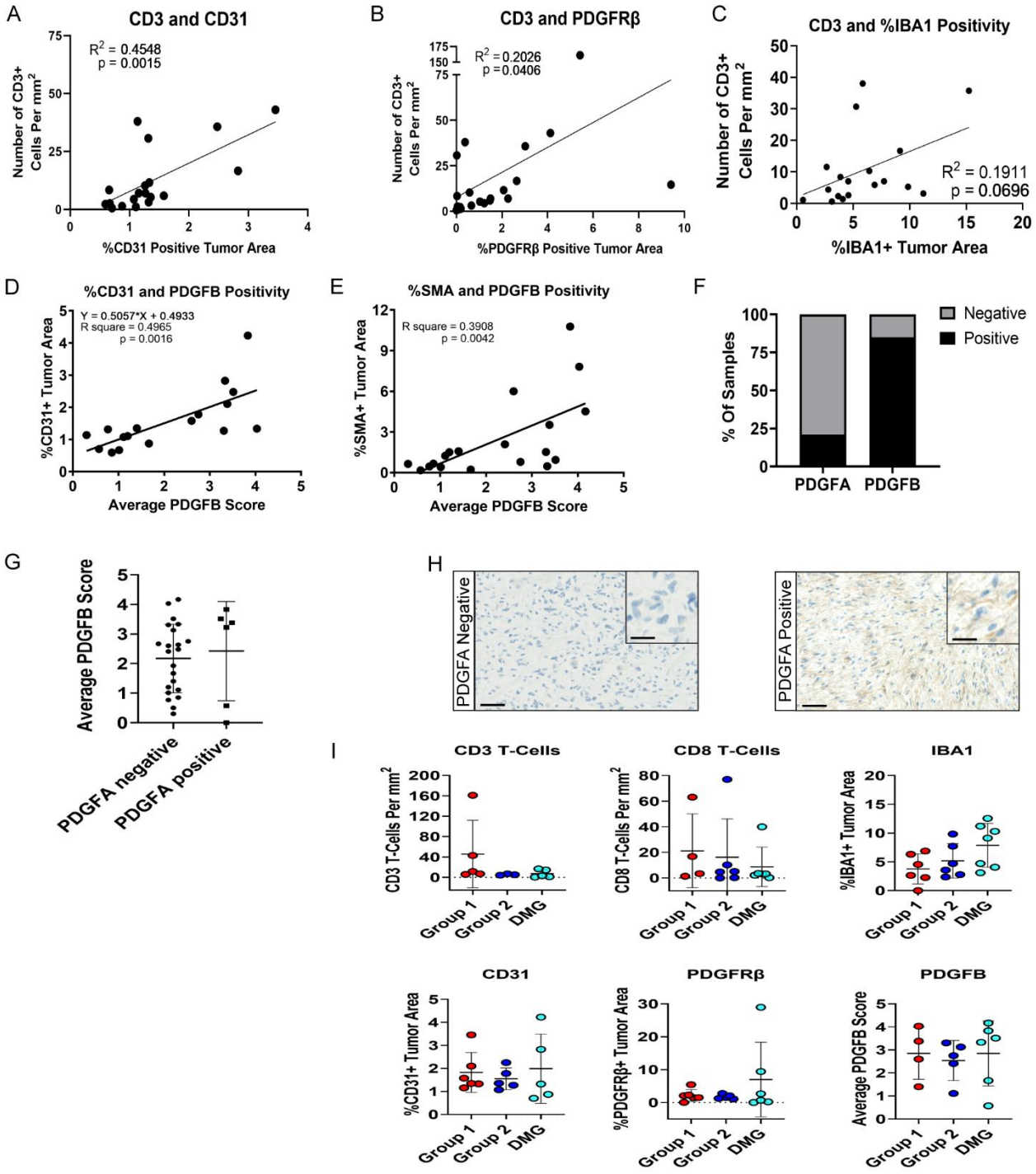

Figure 2. (A) Correlation between CD3 and CD31 immunohistochemical staining in human pHGG samples. **(B)** Correlation between CD3 and PDGFRb staining in human pHGG samples. **(C)** Correlation between CD3 and IBA1 staining in human pHGG samples. **(D)** PDGFB positivity obtained from human pHGG tissue staining correlated with %CD31+ tumor area and **(E)** %SMA+ tumor area in matched samples. **(F)** Percent of human samples positively or

negatively stained for PDGFA and PDGFB ligands. There was no correlation between PDGFA and PDGFB staining. **(G)** Samples that stained negatively or positively for PDGFA and their corresponding PDGFB staining score. 7 out of 33 samples positively stained for PDGFA, and there was no correlation between PDGFA and PDGFB staining. **(H)** Negative and positive PDGFA staining in human pHGG samples. **(I)** IHC quantifications for the indicated markers, categorized by human hemispheric pHGG group 1 (more inflammatory), hemispheric pHGG group 2 (less inflammatory), and DMG. Only samples that had both NanoString and IHC done were included.

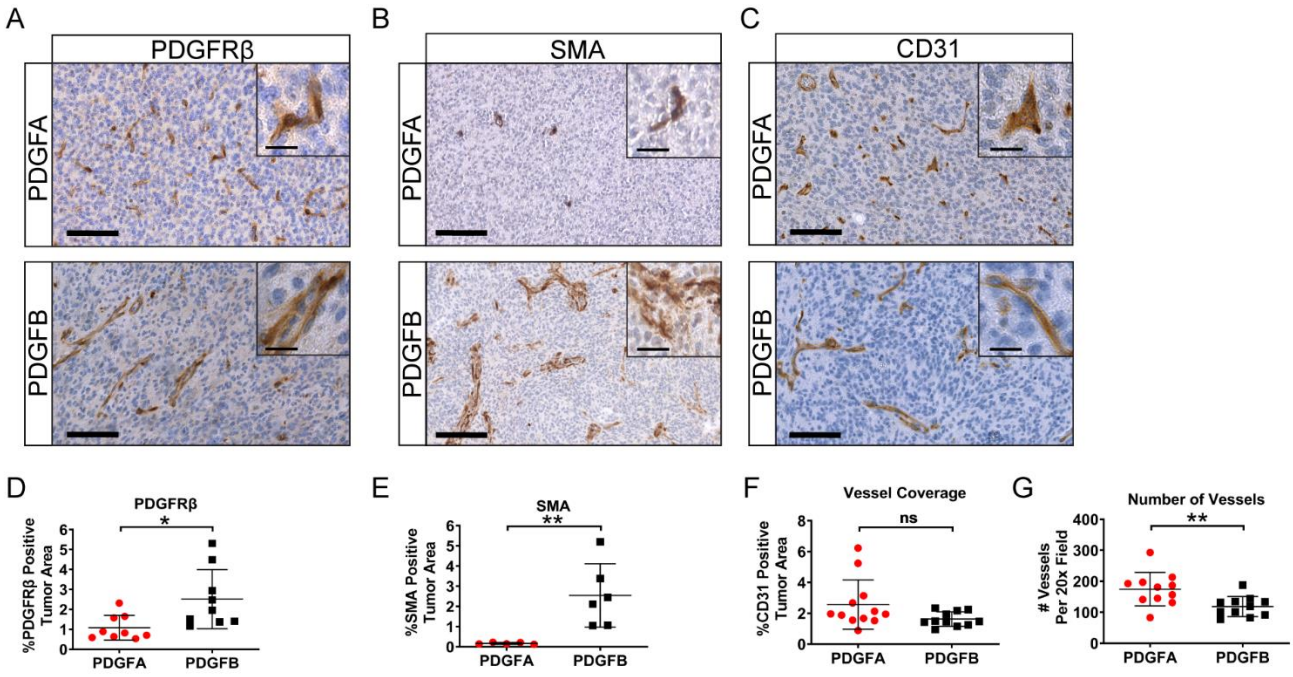

Figure 3. Representative immunohistochemical staining images from hemispheric tumors driven by PDGFA or PDGFB in *Ntva;Cdkn2a*$^{-/-}$ mice. **(A)** PDGFRβ staining. **(B)** Smooth muscle actin (SMA) staining. **(C)** CD31 staining. **(D)** Quantification of PDGFRβ staining. **(E)** Quantification of SMA staining. **(F)** Quantification of vessel coverage as indicated by CD31 staining. **(G)** Quantification of the number of blood vessels detected by CD31 staining. All representative images (a, b, c) are 20x with 80x magnified insets, scale bar=20μm and 100μm respectively. Students *t*-test, *p<0.05, **p<0.01.

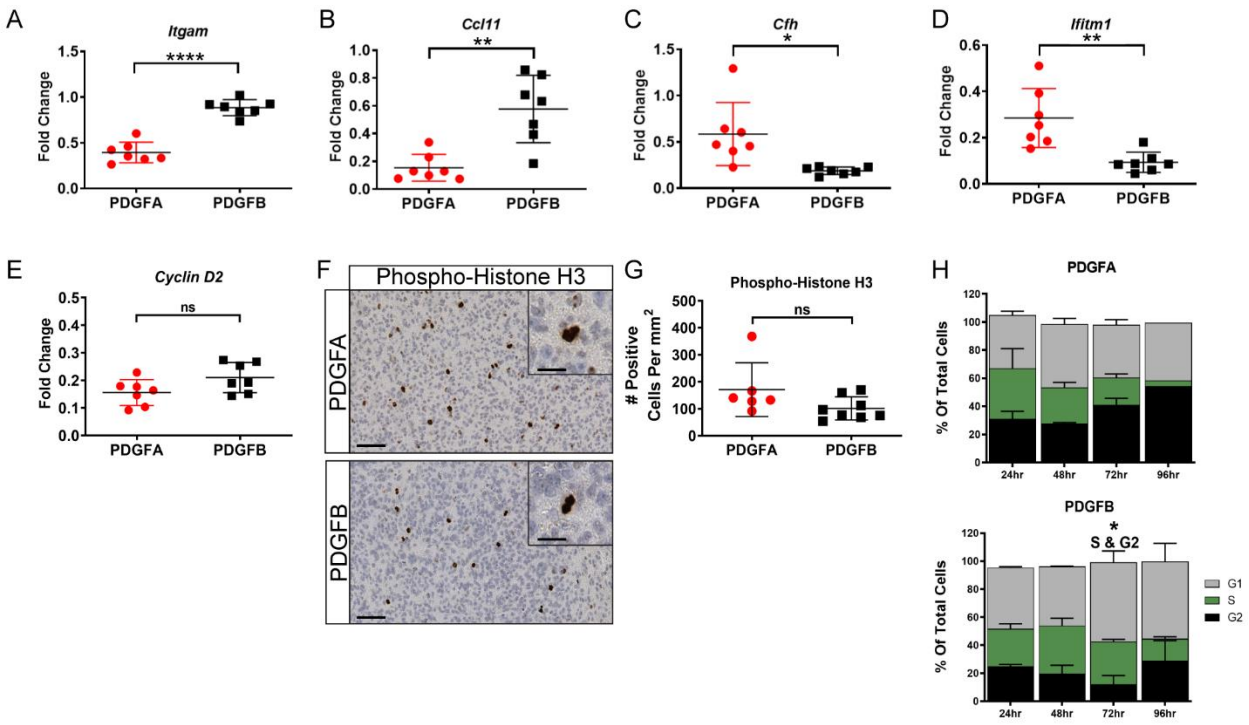

Figure 4. (A-D) qPCR validation of top differentially expressed genes found in NanoString analysis of PDGFA (n=7) and PDGFB-driven (n=7) tumors induced in *Ntva;Cdkn2a*$^{-/-}$ mice. **(E)** qPCR of *Cyclin D2* in PDGFA or PDGFB-driven tumors. **(F-G)** Phospho-histone H3 immunohistochemical staining and quantification. 40x with 80x magnified insets, scale bar=20μm and 100μm respectively. **(H)** Edu proliferation assay results for PDGFA primary cell lines (n=3) and PDGB primary cell lines (n=2) at 24hr, 48hr, 72hr, and 96hrs. Students *t*-test, *p<0.05, **p<0.01, ****p<0.0001.

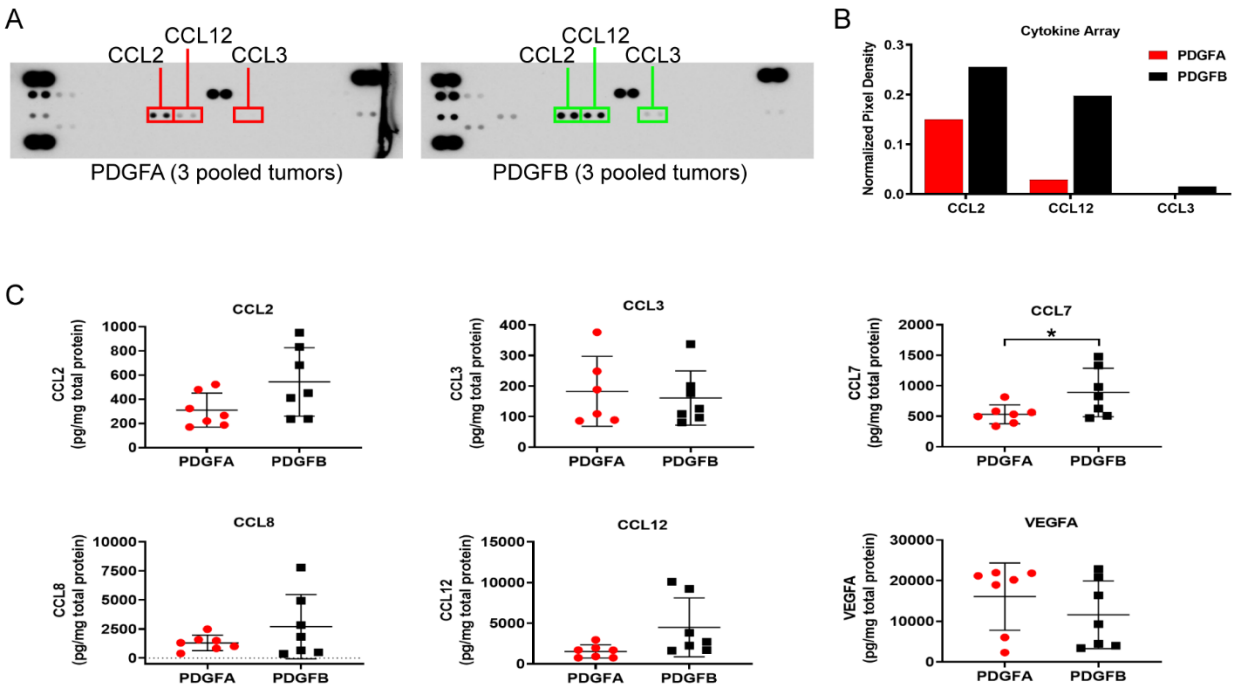

Figure 5. (A) Cytokine array of 3 pooled PDGFA tumor samples and 3 pooled PDGFB tumor samples. CCL2, CCL3, and CCL12 are all highlighted. **(B)** Quantification of pixel intensity for CCL2, CCL3, and CCL12 from the cytokine array. **(C)** Protein ELISA performed on PDGFA (n=7) and PDGFB (n=7) tumor samples for CCL2, CCL3, CCL7, CCL8, CCL12, and VEGFA**.** Students *t*-test. *p<0.05.

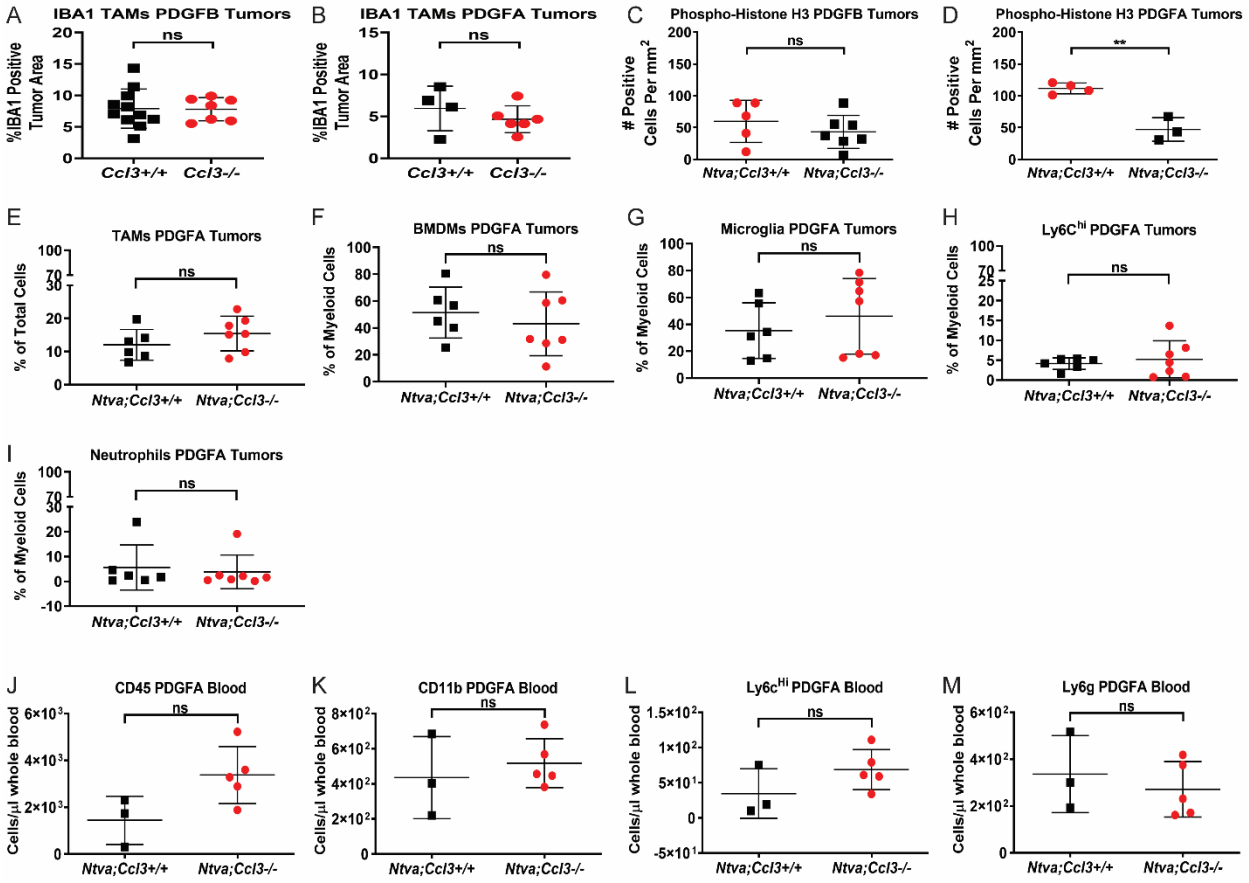

Figure 6. (A-B) Quantification of IBA1+ tumor area in PDGFB or PDGFA-driven tumors in *Ntva;Ccl3+/+* and *Ntva;Ccl3-/-* mice. **(C-D)** Quantification of Phospho-histone H3 staining in PDGFB and PDGFA-driven tumors in *Ntva;Ccl3+/+* and *Ntva;Ccl3-/-* mice. **(E-I)** Quantification of myeloid cell populations via flow cytometry in PDGFA-driven tumors in *Ntva;Ccl3+/+* and *Ntva;Ccl3-/-* mice. **(J-M)** Quantification of myeloid cell populations in the blood of PDGFA-driven tumors in *Ntva;Ccl3+/+* and *Ntva;Ccl3-/-* mice.

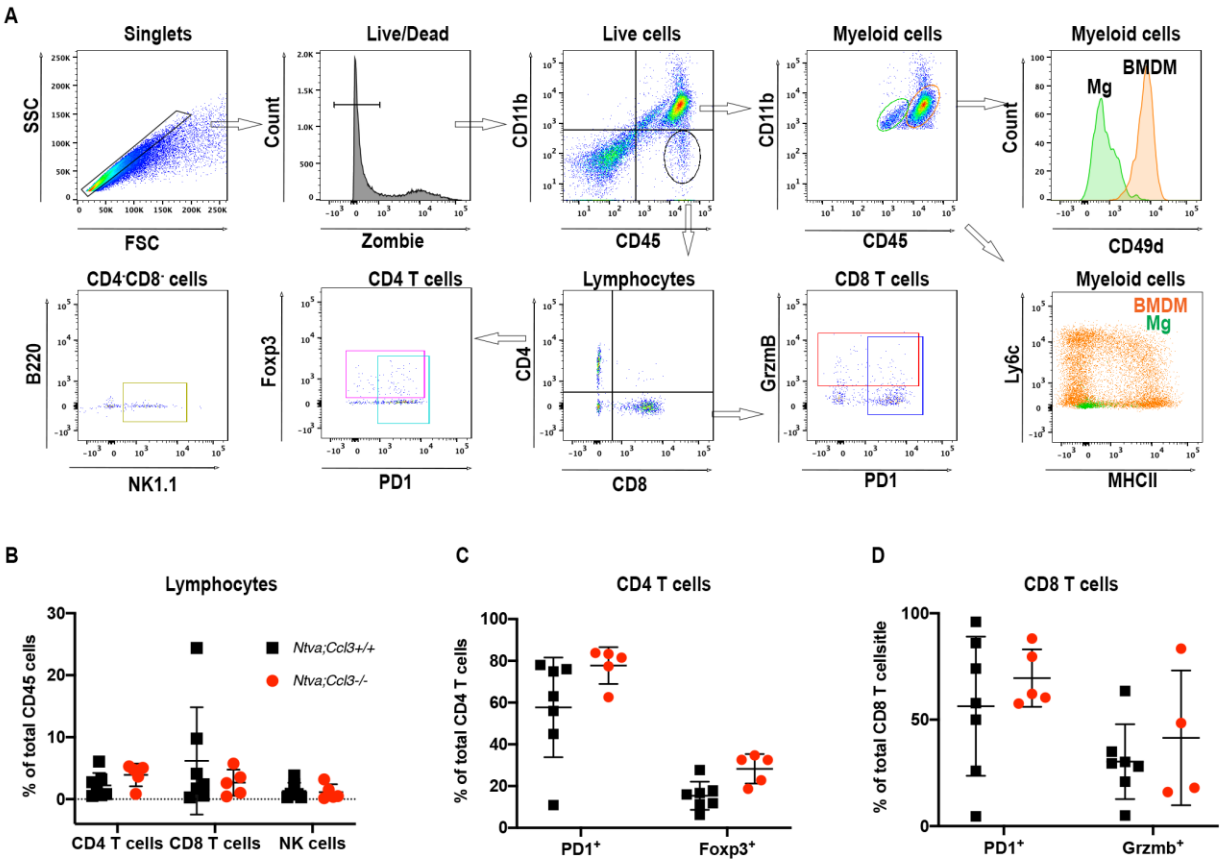

Figure 7. (A) Gating strategy for the analysis of intratumoral innate and adaptive cell infiltrates in PDGFB-driven tumors in *Ntva;Ccl3+/+* and *Ntva;Ccl3-/-* mice. **(B)** Quantification of CD4 T-cells, CD8 T-cells, and NK cells in PDGFB-driven tumors in *Ntva;Ccl3+/+* and *Ntva;Ccl3-/-* mice. **(C)** Quantification of PD1+ or FOXP3+ CD4 T-cells. **(D)** Quantification of PD1+ or Granzyme B+ CD8 T-cells. There were no significant differences found between WT and KO tumors for all comparisons in Figure 7B-D.

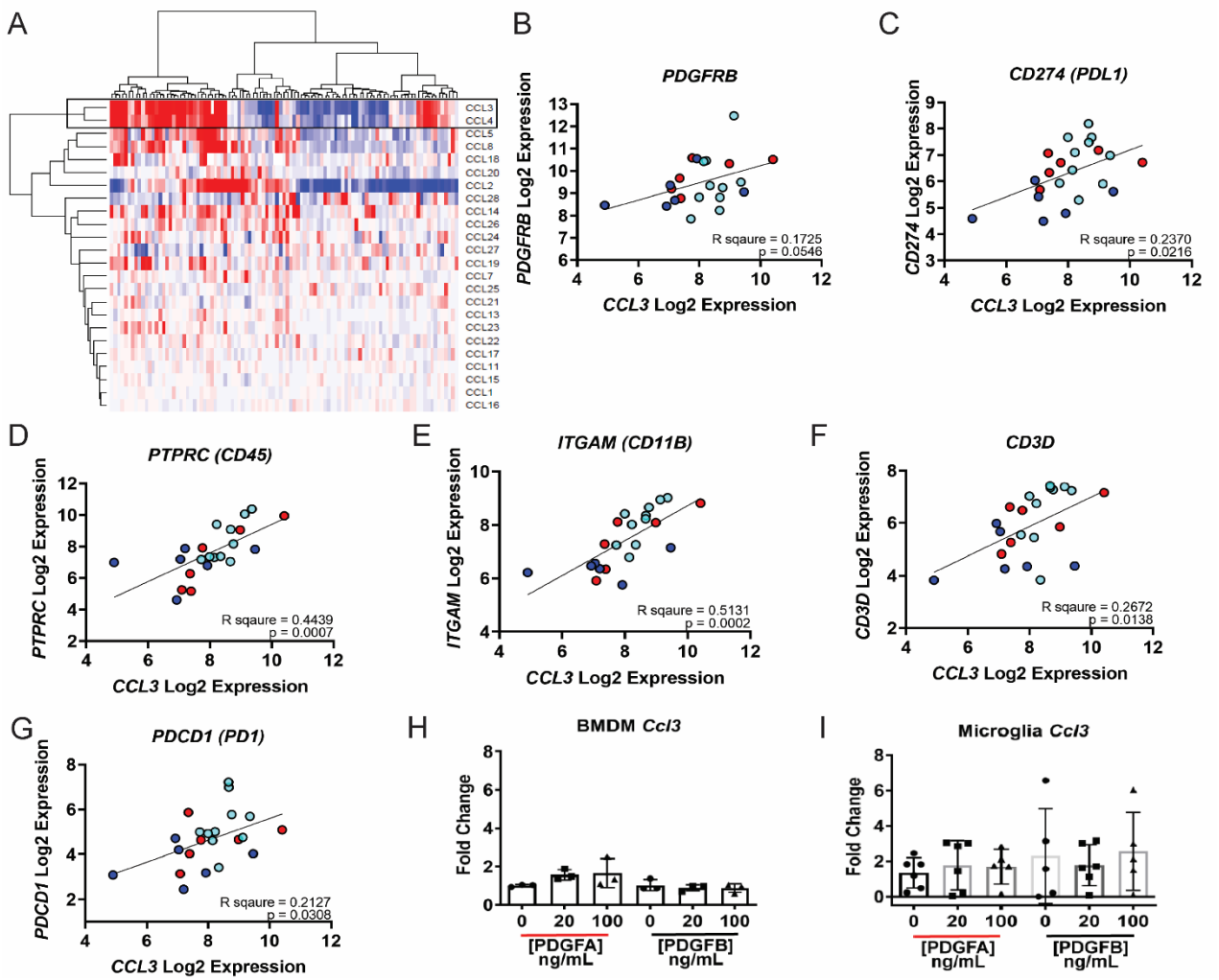

Figure 8. (A) Unsupervised hierarchical clustering of chemokines in human histone WT pHGG RNA sequencing data. n=101. **(B-G)** *CCL3* expression correlated with *PDGFRB, CD274, PTPRC, ITGAM, CD3D, and PDCD1* expression in our human pHGG NanoString dataset. Samples color coded by Group 1 hemispheric tumors (red), Group 2 hemispheric tumors (dark blue), or DIPG (light blue). n=22. **(H-I)** Primary BMDM or microglial cell cultures were stimulated with recombinant PDGFA or PDGFB for 6 hours and qPCR for *Ccl3* was performed. No significant differences were observed.

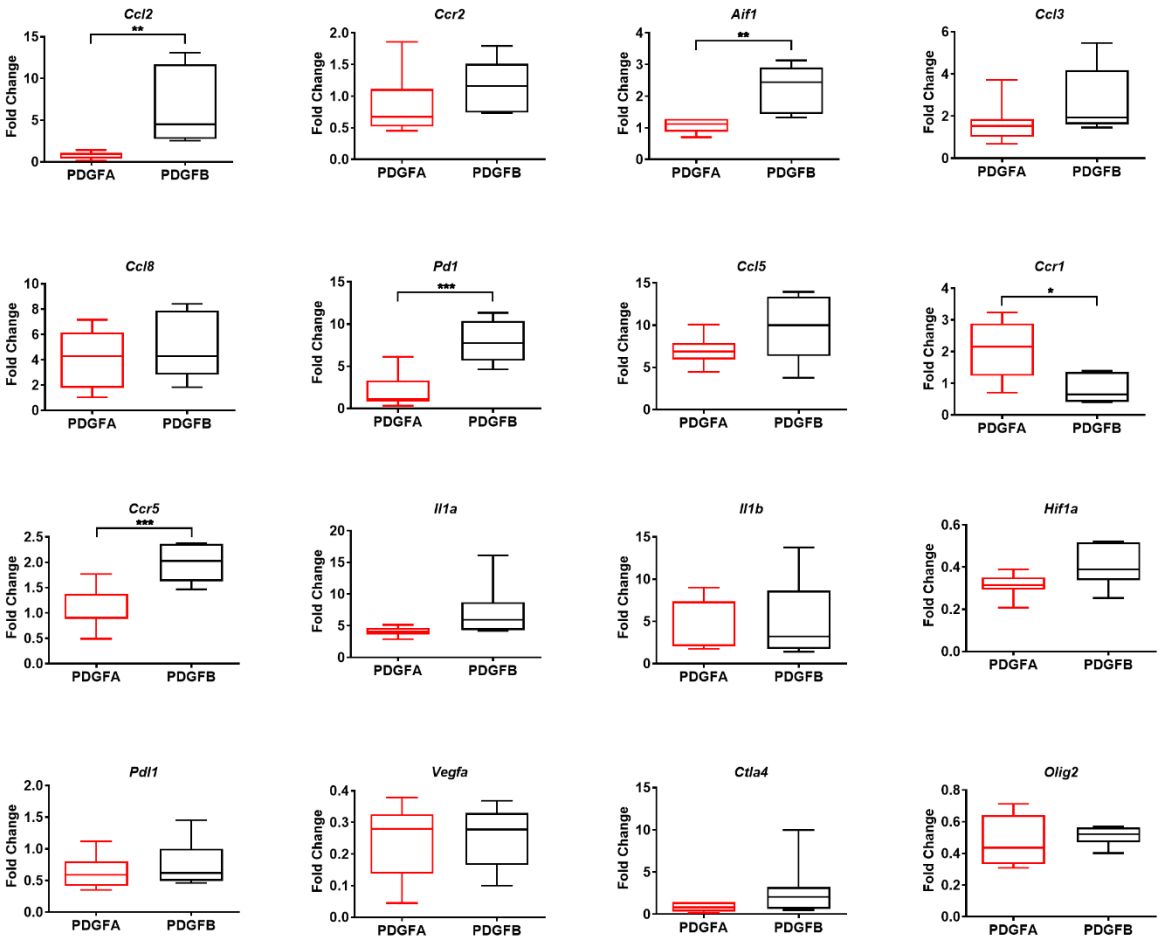
Ccl2
**
Fold Change
15
10
5
0
PDGFA
PDGFB
Ccr2
Fold Change
2.0
1.5
1.0
0.5
0.0
PDGFA
PDGFB
Aif1
**
Fold Change
4
3
2
1
0
PDGFA
PDGFB
Ccl3
Fold Change
6
4
2
0
PDGFA
PDGFB
Ccl8
Fold Change
10
8
6
4
2
0
PDGFA
PDGFB
Pd1
***
Fold Change
15
10
5
0
PDGFA
PDGFB
Ccl5
Fold Change
15
10
5
0
PDGFA
PDGFB
Ccr1
*
Fold Change
4
3
2
1
0
PDGFA
PDGFB
Ccr5
***
Fold Change
2.5
2.0
1.5
1.0
0.5
0.0
PDGFA
PDGFB
Il1a
Fold Change
20
15
10
5
0
PDGFA
PDGFB
Il1b
Fold Change
15
10
5
0
PDGFA
PDGFB
Hif1a
Fold Change
0.6
0.4
0.2
0.0
PDGFA
PDGFB
Pdl1
Fold Change
2.0
1.5
1.0
0.5
0.0
PDGFA
PDGFB
Vegfa
Fold Change
0.4
0.3
0.2
0.1
0.0
PDGFA
PDGFB
Ctla4
Fold Change
15
10
5
0
PDGFA
PDGFB
Olig2
Fold Change
0.8
0.6
0.4
0.2
0.0
PDGFA
PDGFB

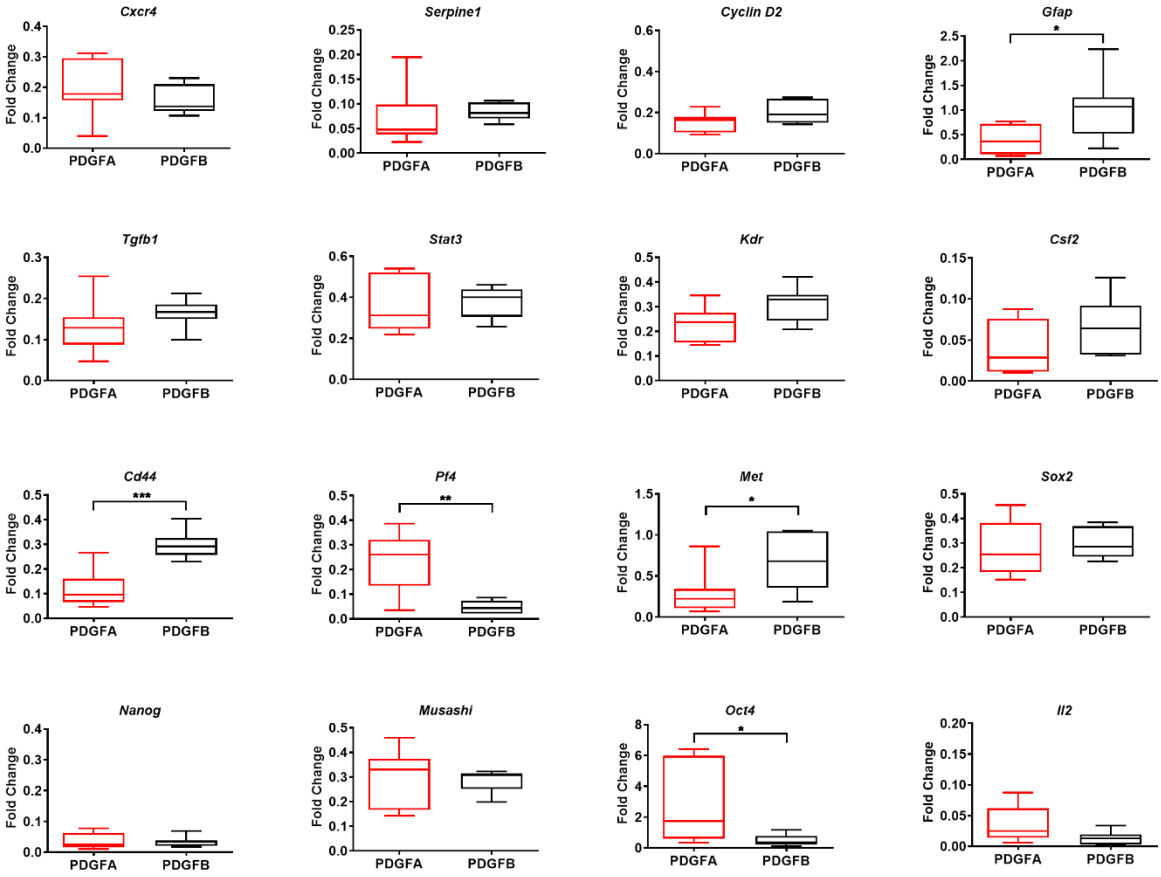
Cxcr4
Fold Change
0.4
0.3
0.2
0.1
0.0
PDGFA
PDGFB
Serpine1
Fold Change
0.25
0.20
0.15
0.10
0.05
0.00
PDGFA
PDGFB
Cyclin D2
Fold Change
0.6
0.4
0.2
0.0
PDGFA
PDGFB
Gfap
*
Fold Change
2.5
2.0
1.5
1.0
0.5
0.0
PDGFA
PDGFB
Tgfb1
Fold Change
0.3
0.2
0.1
0.0
PDGFA
PDGFB
Stat3
Fold Change
0.6
0.4
0.2
0.0
PDGFA
PDGFB
Kdr
Fold Change
0.5
0.4
0.3
0.2
0.1
0.0
PDGFA
PDGFB
Csf2
Fold Change
0.15
0.10
0.05
0.00
PDGFA
PDGFB
Cd44
***
Fold Change
0.5
0.4
0.3
0.2
0.1
0.0
PDGFA
PDGFB
Pf4
**
Fold Change
0.5
0.4
0.3
0.2
0.1
0.0
PDGFA
PDGFB
Met
*
Fold Change
1.5
1.0
0.5
0.0
PDGFA
PDGFB
Sox2
Fold Change
0.5
0.4
0.3
0.2
0.1
0.0
PDGFA
PDGFB
Nanog
Fold Change
0.4
0.3
0.2
0.1
0.0
PDGFA
PDGFB
Musashi
Fold Change
0.5
0.4
0.3
0.2
0.1
0.0
PDGFA
PDGFB
Oct4
*
Fold Change
8
6
4
2
0
PDGFA
PDGFB
Il2
Fold Change
0.20
0.15
0.10
0.05
0.00
PDGFA
PDGFB

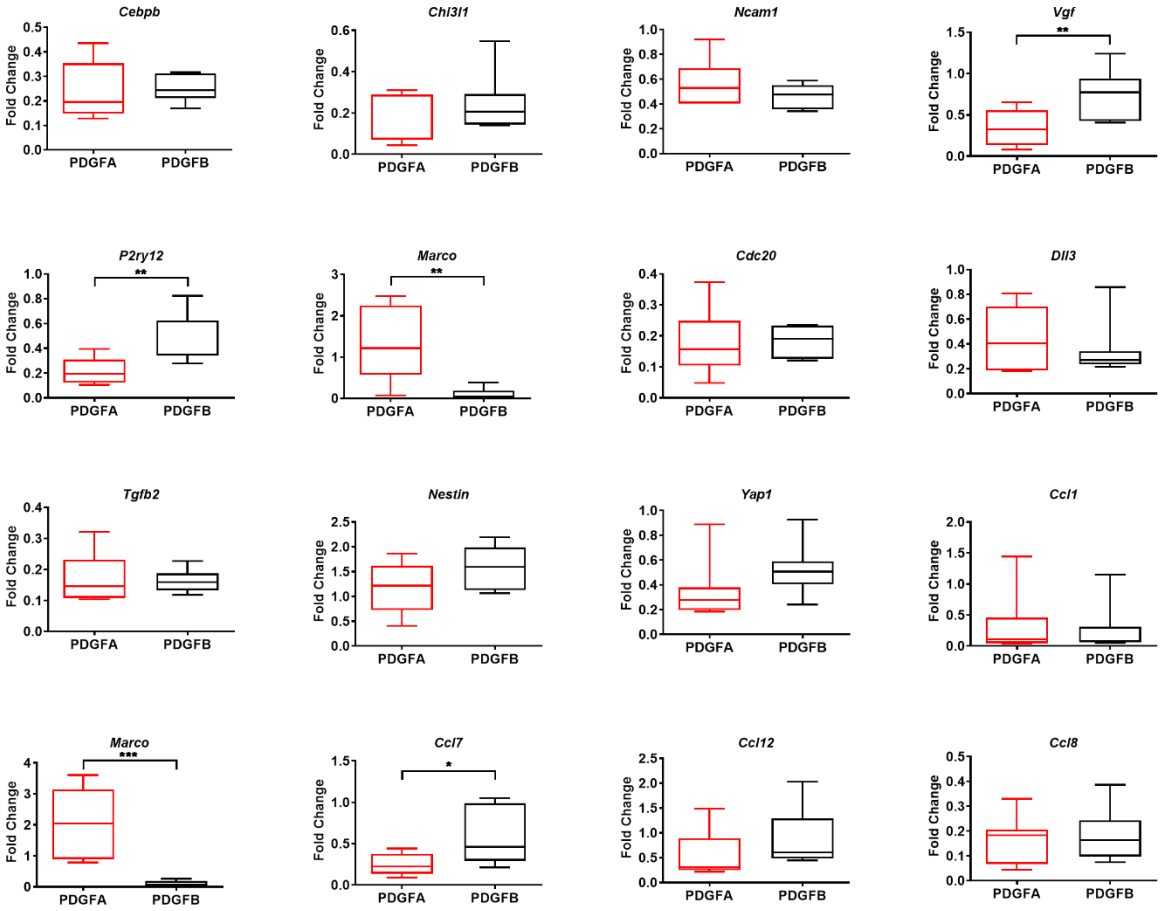
Cebpb
Chl3l1
Ncam1
Vgf
**
P2ry12
**
Marco
**
Cdc20
Dll3
Tgfb2
Nestin
Yap1
Ccl1
Marco
***
Ccl7
*
Ccl12
Ccl8
Fold Change
PDGFA
PDGFB

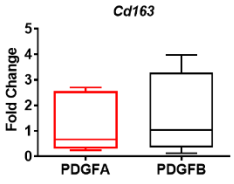
Cd163
Fold Change
PDGFA
PDGFB

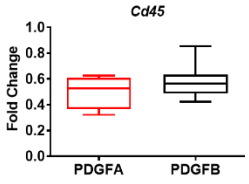
Cd45
Fold Change
PDGFA
PDGFB

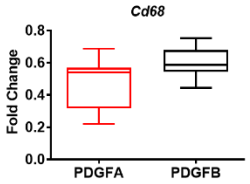
Cd68
Fold Change
PDGFA
PDGFB

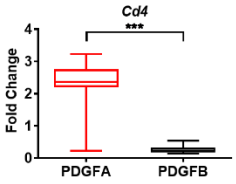
Cd4
***
Fold Change
PDGFA
PDGFB

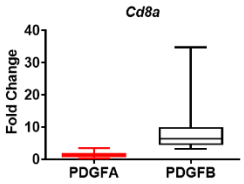
Cd8a
Fold Change
PDGFA
PDGFB

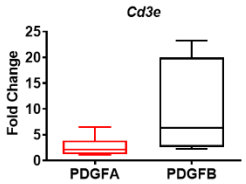
Cd3e
Fold Change
PDGFA
PDGFB

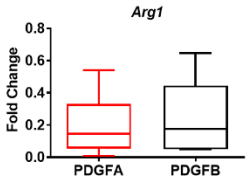
Arg1
Fold Change
PDGFA
PDGFB

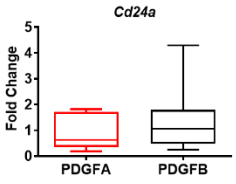
Cd24a
Fold Change
PDGFA
PDGFB

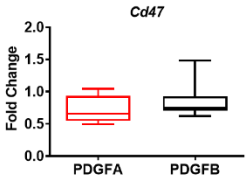
Cd47
Fold Change
PDGFA
PDGFB

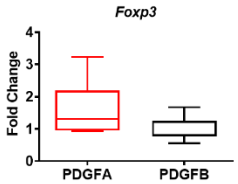
Foxp3
Fold Change
PDGFA
PDGFB

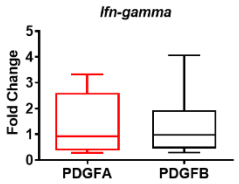
Ifn-gamma
Fold Change
PDGFA
PDGFB

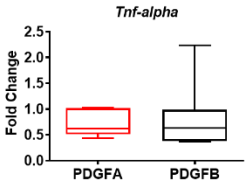
Tnf-alpha
Fold Change
PDGFA
PDGFB

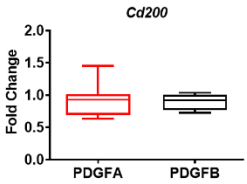
Cd200
Fold Change
PDGFA
PDGFB

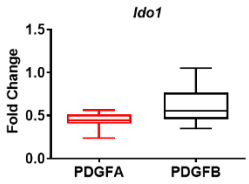
Ido1
Fold Change
PDGFA
PDGFB

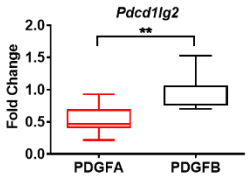
Pdcd1lg2
**
Fold Change
PDGFA
PDGFB

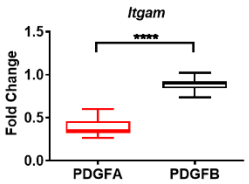
Itgam
****
Fold Change
PDGFA
PDGFB

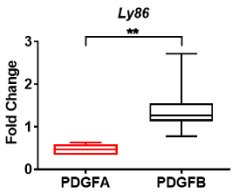
Ly86
**
Fold Change
PDGFA
PDGFB

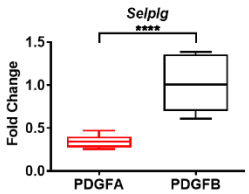
Selplg
****
Fold Change
PDGFA
PDGFB

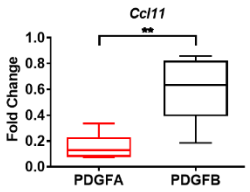
Ccl11
**
Fold Change
PDGFA
PDGFB

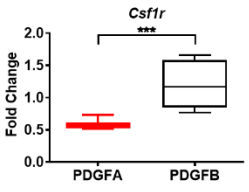
Csf1r
***
Fold Change
PDGFA
PDGFB

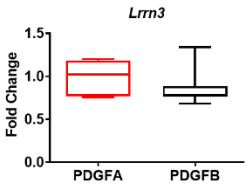
Lrrn3
Fold Change
PDGFA
PDGFB

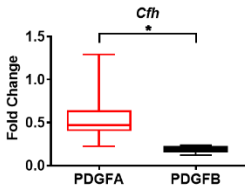
Cfh
*
Fold Change
PDGFA
PDGFB

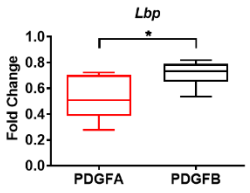
Lbp
*
Fold Change
PDGFA
PDGFB

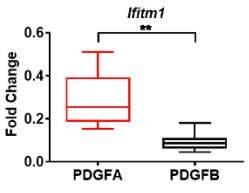
Ifitm1
**
Fold Change
PDGFA
PDGFB

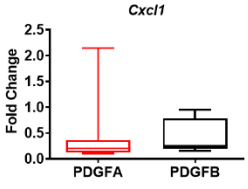
Cxcl1
Fold Change
PDGFA
PDGFB

Figure 9. Box plots of all genes run on PDGFA (n=7) and PDGFB-driven (n=7) pHGG tumors in *Ntva;Cdkn2a*$^{-/-}$ mice.

Sample ID	Diagnosis	Tumor Location	Age at Dx (Mos)	Survival (Weeks since Dx)	Sex	Treatment	Molecular Characteristics	Nano-String
PGBM 1	DIPG	Pons	69.87	47.00	F	-	-	Y
PGBM 2	DIPG	Pons	40.83	94.29	F	-	-	Y
PGBM 3	AA	Temporal, left	112.77	43.14	M	-	PIK3CA:p.H1047R mut. Loss of CDKN2A	Y
PGBM 4	DIPG	Pons, lateral	114.80	65.86	M	-	EGFR amp, CDK6 amp	Y
PGBM 5	GBM	Basal ganglia, right	6.50	29.57	F	-	-	Y
PGBM 6	GBM	Frontal, right	145.33	40.43	M	-	PIK3CA:p.H1047R mut. Loss of CDKN2A	Y
PGBM 7	DIPG	Pons	76.00	34.57	F	-	-	N
PGBM 8	DIPG	Pons	119.27	59.14	F	-	-	N
PGBM 9	GBM	Pons	41.60	48.86	F	-	-	N
PGBM 10	DIPG	Pons	55.53	85.43	F	-	-	Y
PGBM 11	GBM	Frontal, right	203.30	20.29	M	-	MET-PTPRZ1 gene fusion	Y
PGBM 12	DIPG	Pons	88.03	76.86	M	-	-	Y
PGBM 13	GBM	Temporal, left	141.67	67.71	M	Radiation	-	Y
PGBM 14	GBM-K27M	-	0.00	0.00	-	-	K27M	N
PGBM 15	AA-G34R	Temporal, Left	206.27	alive	F	-	H3-G34R & TP53 mutations	Y
PGBM 16	Thalamic K27M	Thalamus/frontal, right	187.50	15.14	M	-	K27M	Y
PGBM 17	DIPG-K27M	Pons	48.93	155.86	M	-	K27M	N
PGBM 18	DIPG-K27M	Pons	149.20	249.43	F	-	K27M	N
PGBM 19	GBM	Parietal, right	194.87	31.29	M	Radiation	-	Y
PGBM 20	GBM	Parietal, right	164.93	45.86	F	Radiation	-	Y
PGBM 21	GBM-K27M	Thalamus, left	67.13	41.00	M	-	K27M	Y
PGBM 22	GBM	Frontal, right	183.33	alive	M	Radiation	-	Y
PGBM 23	GBM	Temporal, left	204.60	283.43	M	Radiation	-	Y
PGBM 24	GBM	Temporal, left	173.73	84.43	M	-	EGFR amp, PTEN loss	Y
PGBM 25	GBM-K27M	Thalamus, left	179.23	75.14	M	-	K27M	Y
PGBM 26	GBM-G34R	Temporal, left	157.37	126.29	M	-	H3 G34R	Y
PGBM 27	GBM	Right	60.00	9.00	M	-	Amp. MYCN, ampMDM4, ampMIR205	N
PGBM 28	GBM	Right frontoparietal	60.00	17.00	M	-	EGFR amp, CDK6 amp	N
PGBM 29	Anaplastic Ependymoma III	Right hemisphere	180.00	24.00	F	-	-	N
PGBM 30	AA III/IV-G34R/V	Temporal, right	120.00	25.00	M	-	H3 G34V, P53 mut, EGFR gain, CDK6 gain, MET gain, MYCN gain, CDKN2A gain, PTCH1 gain	N

PGBM 31	GBM	Left frontal lobe	60	7	F	-	-	N
PGBM 32	GBM	Left frontal lobe	144	16	M	-	EGFR, TERT, PIK3CA mutations, CDKN2A loss	N
PGBM 33	GBM	Left CP angle near pons	96	11	F	-	-	N
PGBM 34	DIPG	Pons	47.00	152.08	-	-	K27M	N
PGBM 35	DIPG	Pons	39.00	91.25	-	-	K27M	N
PGBM 36	DIPG	Pons	68.00	43.45	-	-	K27M unknown	N
PGBM 37	DIPG	Pons	54.00	82.55	-	-	K27M unknown	N
PGBM 38	DIPG	Pons	146.00	247.67	-	-	K27M	N
PGBM 39	GBM-K27M	Right	-	-	M	-	-	N
PGBM 40	GBM-G34R	Temporo-parietal, right	254.40	alive	M	-	G34R	Y
PGBM 41	AA	Pons	161.90	45.29	M	-	-	N
PGBM 42	AA	Right hemisphere, thalami	213.23	alive	M	-	-	N
PGBM 43	GBM-K27M	Thalamus, right	140.40	79.14	F	-	K27M	N
PGBM 44	DIPG-K27M	Pons	157.20	alive	M	-	K27M	N
PGBM 45	DIPG	Pons	143.77	453.29	M	-	Not K27M	Y
PGBM 46	AA-K27M	Thalami	201.37	59	F	-	K27M	N
PGBM 48	GBM-K27M	Thalamus	-	-	-	-	K27M	Y

Table 1. Patient characteristics of samples used in this study.

Antibody	Application	Host Tissue	Company	Catalog Number
IBA1	IHC	Mouse, Human	Wako	019-19741
PDGFRa	IHC	Mouse	Cell Signaling	CST 3174S
PDGFRb	IHC	Mouse	Cell Signaling	CST 3169S
Phospho Histone 3	IHC	Mouse	Cell Signaling	CST 9701S
CD31	IHC	Mouse	Dianova	DIA-310
Smooth Muscle Actin	IHC	Mouse	Dako	M0851
PDGFA	IHC	Human	Santa Cruz	sc-128
PDGFB	IHC	Human	Santa Cruz	sc-127
PDGFRa	IHC	Human	Cell Signaling	cs3174
PDGFRb	IHC	Human	Cell Signaling	cs3169
CD31	IHC	Human	Dako	M0823
CD3	IHC	Human	Dako	A0452
CD8	IHC	Human	Dako	M7103
CD45-APC	Flow Cytometry	Mouse	BioLegend	103112
CD11b-PerCP-Cy5.5	Flow Cytometry	Mouse	BD Biosciences	550993
Ly6C-PE-Cy7	Flow Cytometry	Mouse	BD Biosciences	560593
Ly6C-BV-650	Flow Cytometry	Mouse	BioLegend	128049
Ly6G-V450	Flow Cytometry	Mouse	BD Biosciences	560603
CD49d-PE-Cy7	Flow Cytometry	Mouse	BioLegend	103617
I-A/I-E-A700	Flow Cytometry	Mouse	BioLegend	107621
CD4-APC-Cy7	Flow Cytometry	Mouse	BioLegend	100526
CD8-BV-510	Flow Cytometry	Mouse	BioLegend	100752
B220-BV-605	Flow Cytometry	Mouse	BioLegend	103243
NK1.1-BV-711	Flow Cytometry	Mouse	BD Biosciences	740663
PD1-BV-785	Flow Cytometry	Mouse	BioLegend	135225
Foxp3-FITC	Flow Cytometry	Mouse	eBiosciences	11-5773-82
GranzymeB-PE	Flow Cytometry	Human/Mouse	eBiosciences	12-8899-41
PDGFAA	Cell Culture Stimulation	Human	R&D	221-AA-010
PDGFBB	Cell Culture Stimulation	Human	R&D	220-BB-010

Table 2. All antibodies used in the study are listed.

Primer	Bio-Rad Catalog Number	Primer	Bio-Rad Catalog Number
Actb	qMmuCED0027505	Pd1	qMmuCID0011570
Cdc20	qMmuCED0005008	Ccr5	qMmuCID0020341
Dll3	qMmuCID0023659	Cd44	qMmuCID0025677
Tgfb2	qMmuCID0024408	Met	qMmuCID0017026
Yap1	qMmuCID0005990	Ccl7	qMmuCED0049027
Mgmt	qMmuCID0009593	Il2	qMmuCED0060978
Ccr8	qMmuCID0006837	Pdl1	qMmuCID0011907
Ctla4	qMmuCID0008808	Pdgfa	qHsaCID0005879
Sox2	qMmuCED0051857	Ccl8	qMmuCED0003781
Oct4	qMmuCED0046525	Ccl5	qMmuCID0021047
Musashi	qMmuCID0040186	Vegfa	qMmuCED0040260
Nanog	qMmuCID0005399	Nestin	qMmuCID0023067
Stat3	qMmuCID0021132	Spp1	qMmuCED0061675
Ccnd2	qMmuCID0023538	Cxcr4	qMmuCED0026325
Cxcr4	qMmuCED0026325	Cxcl12	qMmuCID0019961
Kdr	qMmuCID0005890	Cd8a	qMmuCID0016523
Ncam1	qMmuCID0005870	Foxp3	qMmuCID0022414
Ccl3	qMmuCED0003870	Lbp	qMmuCED0045303
Chi3l1	qMmuCID0015758	Cfh	qMmuCED0045575
Serpine1	qMmuCID0027303	Lrrn3	qMmuCID0019276
Pdgfb	qHsaCID0016004	Csf1r	qMmuCID0016567
Il1a	qMmuCID0005637	Ccl11	qMmuCED0044849
Pf4	qMmuCED0003895	Selplg	qMmuCED0050109
Tgfb1	qMmuCID0017320	Ly86	qMmuCED0045007
Marco	qMmuCID0023893	Itgam	qMmuCID0005971
Csf2	qMmuCED0025728	Pdcd1lg2	qMmuCID0011922
P2ry12	qMmuCID0015382	Ido1	qMmuCED0047121
Vgf	qMmuCED0049363	Cd200	qMmuCED0045566
Gfap	qMmuCID0020163	Tnfa	qMmuCED0004141
Aif1	qMmuCED0046745	Ifng	qMmuCID0006268
Il1b	qMmuCID0005641	Cd47	qMmuCED0049651
Ccr1	qMmuCID0006862	Arg1	qMmuCID0022400
Ccl2	qMmuCED0048300	Cd3e	qMmuCED0047615
Ccl1	qMmuCED0038249	Cd8a	qMmuCID0016523
Olig2	qMmuCED0003760	Cd4	qMmuCID0022320
Cebpb	qMmuCED0050360	Cd68	qMmuCED0003822

Ccr1	qMmuCID0006862	Cd45 (Ptprc)	qMmuCID0039693
Ccl12	qMmuCED0061017	Cd163	qMmuCID0012017

Table 3. qPCR Primers Used in Study. The Bio-Rad qPCR primers used in the study are listed with their catalog numbers.

Chen Z, Herting CJ, Ross JL, Gabanic B, Puigdelloses Vallcorba M, Szulzewsky F, *et al.* Genetic driver mutations introduced in identical cell-of-origin in murine glioblastoma reveal distinct immune landscapes but similar response to checkpoint blockade. Glia 2020.
Herting CJ, Chen Z, Maximov V, Duffy A, Szulzewsky F, Shayakhmetov DM, *et al.* Tumour-associated macrophage-derived interleukin-1 mediates glioblastoma-associated cerebral oedema. Brain 2019.
Mackay A, Burford A, Carvalho D, Izquierdo E, Fazal-Salom J, Taylor KR, *et al.* Integrated Molecular Meta-Analysis of 1,000 Pediatric High-Grade and Diffuse Intrinsic Pontine Glioma. Cancer Cell 2017; 32(4): 520-37 e5.